

Performance Comparison Of UPFC In Coordination With Optimized POD And PSS On Damping Of Power System Oscillations

S. N. DHURVEY , V.K. CHANDRAKAR

Dept. of Electrical Engg,

G.H. Rasoni College of Engineering,

CRPF Gate No.3, Digdoh Hills, Hingna Road, Nagpur,

INDIA

sonal_nd2000@yahoo.co.in, vc_vkc@yahoo.co.in

Abstract: - This paper presents a new approach for determining the effective control signals for damping of oscillations by performance comparison of Unified Power Flow Controller in coordination with Power Oscillation Damping Controller and Power System Stabilizer. For the analysis Modified Phillips-Heffron Model of Single Machine Infinite Bus system is established with Unified Power Flow Controller. Impact of additional damping controllers like Power Oscillation Damping Controller and Power System Stabilizer are designed to achieve improved damping performance of the Single Machine Infinite Bus system by selecting effective control signals. The Power Oscillation Damping Controller parameters are optimized by using Nonlinear Control design Blockset (NCD). Investigations reveal that coordinated tuning of Unified Power Flow Controller with optimized POD parameters provide the robust dynamic performance. Eigen value analysis provides the quantitative measure for the comparative performance of additional damping signal with effective control signals

Key-Words: - FACTS, UPFC, POD, PSS, Damping of oscillations

1 Introduction

The deregulation and competitive environment in the contemporary power networks [1,2] will imply a new scenario in terms of load and power flow condition and so causing problems of line transmission capacity. But nowadays some problems exists like power system oscillation stability refers to the damping of electromechanical oscillations occurring in power systems with oscillation frequency in the range of 0.2 Hz. to 2 Hz. These low-frequency oscillations are the consequence of the development of interconnection of large power systems. A low frequency oscillation in a power system constrains the capability of power transmission, threatens system security and damages the efficient operation of the power system. In recent years, the fast progress in the field of power electronics has opened new opportunities for the power industry via utilization of the controllable Flexible AC Transmission System devices like Unified Power Flow Controller which offer an alternative means to mitigate power system oscillations. Oscillation Stability analysis and control has been an important subject in power system research and applications. To increase power

system oscillation stability, the installation of supplementary excitation control, Power System Stabilizer, is a simple, effective and economical method. Power System Stabilizer [3] is the conventional damping controller applied at generating station along with Automatic Voltage Regulator Control, whereas proposed Power Oscillation Damping Controller can be applied at Unified Power Flow Controller location. Moreover Unified Power Flow Controller further improves the dynamic performance of the power system in coordination with damping controllers. They can improve system operation because they allow for more accurate control of the power flow, better and faster control of voltage and system stability. As a result one of their applications is the damping of power system oscillations, which recently has been attracting the interest of many researchers [1-11]. First phase of research in this area was focussed on developing steady state and dynamic models of the Unified Power Flow Controller proposing control strategy and studies related to system stability enhancement. Wang [4] have proposed a control strategy in which the relative effectiveness of Unified Power Flow Controller control signals in damping low frequency oscillations has been

examined. However they have not presented an approach for obtaining the simultaneous coordination of the Unified Power Flow Controller with each control signal with Power Oscillation Damping Controller and Power System Stabilizer for damping of power system oscillations. Tambey et al [6] have presented a comprehensive approach for the design of UPFC controllers for a SMIB system. However they have not presented an approach for obtaining the simultaneous coordination of UPFC with each control signal with PSS. Dhurvey et al [7] has addressed the effective control signals for SMIB system for simultaneous coordination of UPFC and POD. However they have not optimized the parameters. A potential advantage of the radial basis function network (RBFN) is its ability to implement with less computational burden, there by, making it attractive for real time application. Chandrakar et al [8] presents a design of Proportional Integral (PI) and RBFN controllers for the UPFC in single machine infinite bus system and multi-machine test system to achieve the increase in power handling capacity of the line, improvement in transient stability and damping of oscillations. However they have not optimised the parameters of damping control schemes like POD. As the system performance changes with the UPFC locations, hence the second phase of research has laid more stress on identification of suitable location for UPFC installation. Chaudhary et al [9] has proposed a sensitivity-based approach for identifying the most suitable location for UPFC placement based on the reduction in the severity of a load bus under line outage contingencies which has been tested on IEEE 30 bus system. Ashwani Kumar [10] has proposed mixed integer non-linear programming approach for optimal location of UPFC to enhance loadability of power systems in deregulated electricity environment. A comparative study of UPFC with other FACTS controllers Thyristor Controlled Phase Angle Regulator (TCPAR) and Thyristor Controlled Series Capacitor (TCSC) has been presented for enhancement of system loadability for pool as well as hybrid model. Dubey et al [11] presents a systematic approach for the simultaneous tuning of GA based PSS and conventionally tuned PSS for damping local and interarea modes of oscillations effectively. In view of above, the main objectives of this paper are to improve the dynamic performance of the system by using the UPFC in coordination with Optimized POD parameters and PSS independently by using Nonlinear Control Design Blockset (NCD).

2. System Model

System considered for analysis is a Single-Machine Infinite Bus power system installed with a Unified Power Flow Controller in one of the two transmission lines which consists of an excitation transformer, a boosting transformer, two three-phase Gate Turn Off based voltage source converters and a DC link capacitor is shown in Fig.1. Control signals for shunt voltage source converter (VSC-E) are modulation index of the shunt converter (m_E) and phase angle of the shunt-converter voltage (δ_E) and for series voltage source converter (VSC-B) are modulation index of series converter (m_B) and phase angle of the injected voltage (δ_B). The static excitation system, model type IEEE-ST1 A has been considered. The Unified Power Flow Controller is assumed to be based on pulse width modulation converters [4,5]. The nominal loading condition and system parameters are given in Appendix-A

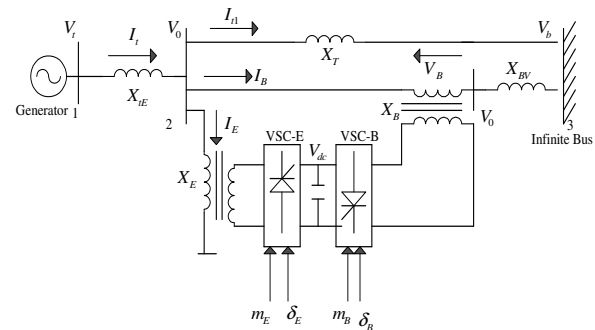


Fig. 1: A single machine infinite bus power system installed with an UPFC in one of the lines

3. Unified Power Flow Controller

Unified Power Flow Controller consists of two voltage source converters. These back-to-back voltage source converters, labeled as voltage source converter with excitation transformer (VSC-E) and voltage source converter with boosting transformer (VSC-B) are operated from a common dc link provided by a dc storage capacitor. This arrangement functions as an ideal ac-to-ac power converter in which the real power can freely flow in either direction between the ac terminals of the two converters, and each converter can independently generate (or absorb) reactive power at its own ac output terminal. The real power output of the shunt converter must be equal to the real power input of the series converter or vice versa. In order to maintain the power balance between the two converters, a DC-voltage regulator is incorporated. DC-voltage is regulated by modulating the phase

angle of the shunt-converter voltage. By applying Park's Transformation, the three-phase dynamic equations of the UPFC are as shown below [2].

$$\begin{bmatrix} \frac{di_{Ea}}{dt} \\ \frac{di_{Eb}}{dt} \\ \frac{di_{Ec}}{dt} \end{bmatrix} = \begin{bmatrix} \frac{r_E}{L_E} & 0 & 0 \\ 0 & -\frac{r_E}{L_E} & 0 \\ 0 & 0 & -\frac{r_E}{L_E} \end{bmatrix} \begin{bmatrix} i_{Ea} \\ i_{Eb} \\ i_{Ec} \end{bmatrix} + \frac{m_E v_{dc}}{2L_E} \begin{bmatrix} \cos(\alpha + \delta_E) \\ \cos(\alpha + \delta_E - 120^\circ) \\ \cos(\alpha + \delta_E + 120^\circ) \end{bmatrix} + \begin{bmatrix} \frac{1}{L_E} & 0 & 0 \\ 0 & \frac{1}{L_E} & 0 \\ 0 & 0 & \frac{1}{L_E} \end{bmatrix} \begin{bmatrix} v_{Ea} \\ v_{Eb} \\ v_{Ec} \end{bmatrix} \quad (1)$$

$$\begin{bmatrix} \frac{di_{Ba}}{dt} \\ \frac{di_{Bb}}{dt} \\ \frac{di_{Bc}}{dt} \end{bmatrix} = \begin{bmatrix} \frac{r_B}{L_B} & 0 & 0 \\ 0 & -\frac{r_B}{L_B} & 0 \\ 0 & 0 & -\frac{r_B}{L_B} \end{bmatrix} \begin{bmatrix} i_{Ba} \\ i_{Bb} \\ i_{Bc} \end{bmatrix} + \frac{m_B v_{dc}}{2L_B} \begin{bmatrix} \cos(\alpha + \delta_B) \\ \cos(\alpha + \delta_B - 120^\circ) \\ \cos(\alpha + \delta_B + 120^\circ) \end{bmatrix} + \begin{bmatrix} \frac{1}{L_B} & 0 & 0 \\ 0 & \frac{1}{L_B} & 0 \\ 0 & 0 & \frac{1}{L_B} \end{bmatrix} \begin{bmatrix} v_{Ba} \\ v_{Bb} \\ v_{Bc} \end{bmatrix} \quad (2)$$

$$\frac{dv_{dc}}{dt} = \frac{m_E}{2C_{dc}} [\cos(\omega t + \delta_E) \cos(\omega t + \delta_E - 120^\circ) \cos(\omega t + \delta_E + 120^\circ)] \begin{bmatrix} i_{Ea} \\ i_{Eb} \\ i_{Ec} \end{bmatrix} + \frac{m_B}{2C_{dc}} [\cos(\alpha + \delta_B) \cos(\alpha + \delta_B - 120^\circ) \cos(\alpha + \delta_B + 120^\circ)] \begin{bmatrix} i_{Ba} \\ i_{Bb} \\ i_{Bc} \end{bmatrix} \quad (3)$$

By ignoring the resistance and transients of the transformers of the UPFC, the equations become

$$\begin{bmatrix} V_{Etd} \\ V_{Etdq} \end{bmatrix} = \begin{bmatrix} 0 & -x_E \\ x_E & 0 \end{bmatrix} \begin{bmatrix} i_{Ed} \\ i_{Eq} \end{bmatrix} + \begin{bmatrix} \frac{m_E \cos \delta_E v_{dc}}{2} \\ \frac{m_E \sin \delta_E v_{dc}}{2} \end{bmatrix} \quad (4)$$

$$\begin{bmatrix} V_{Btd} \\ V_{Btdq} \end{bmatrix} = \begin{bmatrix} 0 & -x_E \\ x_E & 0 \end{bmatrix} \begin{bmatrix} i_{Bd} \\ i_{Bq} \end{bmatrix} + \begin{bmatrix} \frac{m_B \cos \delta_B v_{dc}}{2} \\ \frac{m_B \sin \delta_B v_{dc}}{2} \end{bmatrix} \quad (5)$$

$$\frac{dv_{dc}}{dt} = \frac{3m_E}{4C_{dc}} [\cos \delta_E \sin \delta_E] \begin{bmatrix} i_{Ed} \\ i_{Eq} \end{bmatrix} + \frac{3m_B}{4C_{dc}} [\cos \delta_B \sin \delta_B] \begin{bmatrix} i_{Bd} \\ i_{Bq} \end{bmatrix} \quad (6)$$

$$V_t = jx_{tE} I_t + V_{Et} \quad (7)$$

$$V_{Et} = V_{Bt} + jx_{BV} I_B + V_b \quad (8)$$

Above expressions can be expressed on the d-q coordinate as

$$v_{dt} + jv_{qt} = jx_{tE}(i_{Ed} + i_{Bd} + ji_{Eq} + ji_{Bq}) + v_{Etd} + jv_{Etdq} \quad (9)$$

$$= x_q (i_{Eq} + i_{Bq}) + j [E_q^1 - x_d^1 (i_{Ed} + i_{Bd})] \quad (10)$$

$$v_{Etd} + jv_{Etdq} = v_{Btd} + jv_{Btdq} + jx_{BV} i_{Bd} - jx_{BV} i_{Bq} + V_b \sin \delta + jV_b \cos \delta \quad (11)$$

For the dynamic model of the power system we have

$$T_e = P_e = V_q I_q + V_d I_d \quad (12)$$

$$E_q = E_q^1 + (x_d - x_d^1) i_{dt} \quad (13)$$

$$v_{qt} = E_q^1 - x_d^1 i_{dt} \quad (14)$$

$$v_{dt} = x_q i_{qt} \quad (15)$$

$$v_t = \sqrt{v_{dt}^2 + v_{qt}^2} \quad (16)$$

$$i_{dt} = i_{Ed} + i_{Bd} \quad (17)$$

$$i_{qt} = i_{Eq} + i_{Bq} \quad (18)$$

A linear dynamic model of UPFC is obtained by linearizing the non-linear model around an operating condition as shown below [6].

$$\Delta \dot{\omega} = \frac{(\Delta P_m - \Delta P_e - D \Delta \omega)}{M} \quad (19)$$

$$\Delta \dot{\delta} = \omega_0 \Delta \omega \quad (20)$$

$$\Delta \dot{E}_q = \frac{(-\Delta E_q + \Delta E_{fd})}{T_{do}} \quad (21)$$

$$\Delta \dot{E}_{fd} = \frac{-\Delta E_{fd} + K_a (\Delta V_{ref} - \Delta V_t)}{T_a} \quad (22)$$

$$\Delta \dot{V}_{tE} = K_7 \Delta \delta + K_8 \Delta E_q^1 - K_9 \Delta V_{tE} + K_{10} \Delta m_E + K_{11} \Delta \delta_E + K_{12} \Delta m_B + K_{13} \Delta \delta_B \quad (23)$$

$$\Delta P_e = K_4 \Delta \delta + K_5 \Delta E_q^1 + K_{14} \Delta m_E + K_{15} \Delta \delta_E + K_{16} \Delta m_B + K_{17} \Delta \delta_B + K_{18} \Delta V_{tE} \quad (24)$$

$$\Delta E_q = K_1 \Delta \delta + K_2 \Delta E_q^1 + K_{19} \Delta m_E + K_{20} \Delta \delta_E + K_{21} \Delta m_B + K_{22} \Delta \delta_B + K_{23} \Delta V_{tE} \quad (25)$$

$$\Delta V_t = K_3 \Delta \delta + K_6 \Delta E_q^1 + K_{24} \Delta m_E + K_{25} \Delta \delta_E + K_{26} \Delta m_B + K_{27} \Delta \delta_B + K_{28} \Delta V_{tE} \quad (26)$$

Fig.2 shows the modified Phillips-Heffron model of the SMIB system with UPFC installed [4]. The modified Phillips-Heffron model has 28 constants as apposed to 6 constants in the Phillips-Heffron model. These constants are functions of the system parameters and the initial operating condition. The value of the constants of the model are given in Appendix -A.

The control vector u is defined as follows:

$$u = [\Delta m_B \quad \Delta m_E \quad \Delta \delta_B \quad \Delta \delta_E]^T \quad (27)$$

where,

Δm_B - deviation in pulse width modulation index m_B of series converter. By controlling m_B the

magnitude of series-injected voltage can be controlled, $\Delta\delta_B$ – deviation in phase angle of the injected voltage. Δm_E – deviation in pulse width modulation index m_E of the shunt converter. By controlling m_E , the output voltage of the shunt converter is controlled, $\Delta\delta_E$ – deviation in phase angle of the shunt-converter voltage.

It may be noted that K_{pu} , K_{qu} , K_{vu} , K_{cu} are the row vectors defined below [4]:

$$K_{pu} = [K_{pe} \quad K_{p\delta_e} \quad K_{pb} \quad K_{p\delta_b}] \quad (28)$$

$$K_{qu} = [K_{qe} \quad K_{q\delta_e} \quad K_{qb} \quad K_{q\delta_b}] \quad (29)$$

$$K_{vu} = [K_{ve} \quad K_{v\delta_e} \quad K_{vb} \quad K_{v\delta_b}] \quad (30)$$

$$K_{cu} = [K_{ce} \quad K_{c\delta_e} \quad K_{cb} \quad K_{c\delta_b}] \quad (31)$$

The dynamic model of the system in state-space form is obtained from the transfer-function model as:

$$\dot{X} = AX + Bu \quad (32)$$

$$X = [\Delta\delta \quad \Delta\omega \quad \Delta E_q^1 \quad \Delta E_{fd} \quad \Delta V_{dc}]^T \quad (33)$$

$$A = \begin{bmatrix} 0 & \omega_0 & 0 & 0 & 0 \\ \frac{K_1}{M} & 0 & \frac{K_2}{M} & 0 & \frac{K_{pd}}{M} \\ \frac{K_4}{T_{d0}^1} & 0 & \frac{K_3}{T_{d0}^1} & \frac{1}{T_{d0}^1} & \frac{K_{qd}}{T_{d0}^1} \\ \frac{K_a K_5}{T_a} & 0 & \frac{K_a K_6}{T_a} & \frac{1}{T_a} & \frac{K_a K_{fd}}{T_a} \\ K_7 & 0 & K_8 & 0 & -K_9 \end{bmatrix} \quad (34)$$

$$B = \begin{bmatrix} 0 & 0 & 0 & 0 \\ \frac{K_{pe}}{M} & \frac{K_{p\delta_e}}{M} & \frac{K_{pb}}{M} & \frac{K_{p\delta_b}}{M} \\ \frac{K_{qe}}{M} & \frac{K_{q\delta_e}}{M} & \frac{K_{qb}}{M} & \frac{K_{q\delta_b}}{M} \\ \frac{K_a K_{ve}}{T_a} & \frac{K_a K_{v\delta_e}}{T_a} & \frac{K_a K_{vb}}{T_a} & \frac{K_a K_{v\delta_b}}{T_a} \\ K_{ce} & K_{c\delta_e} & K_{cb} & K_{c\delta_b} \end{bmatrix} \quad (35)$$

4. Coordinated Tuning of POD and UPFC

In this section, coordinated tuning of UPFC and POD Controller is suggested for damping of oscillations. In Fig.2, a POD controller is shown which is provided to improve the damping of power system oscillations [6]. The POD controller may be considered as comprising gain K_{DC} , wash out block

and lag-lead compensator. The parameters of the lead-lag compensator are chosen so as to compensate for the phase shift between the control signal and the resulting electrical power deviation. The gain setting of the damping controller is chosen so as to achieve the desired damping ratio of the electromechanical mode. Optimum parameters for the damping controllers are given in Appendix-A. The UPFC controllable signals (m_E , δ_E , m_B and δ_B) can be modulated in order to produce a damping torque. Controllability indices for the different Unified Power Flow Controller controllable parameters are given in Appendix-A. The washout circuit as shown in Fig.2 is provided to eliminate steady-state bias in the output of POD Controller. The T_{ω} must be chosen in the range of 10 to 20. The power-flow controller as shown in Fig.3 regulates the power flow on this line where K_{pp} and K_{pi} are the proportional and integral gain settings of the power-flow controller as shown in Appendix-A.

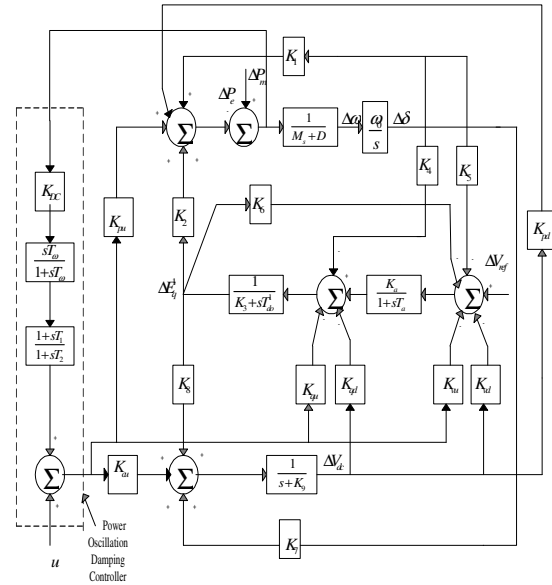


Fig.2: Modified Phillips-Heffron model of SMIB system with Unified Power Flow Controller and Power Oscillation Damping Controller

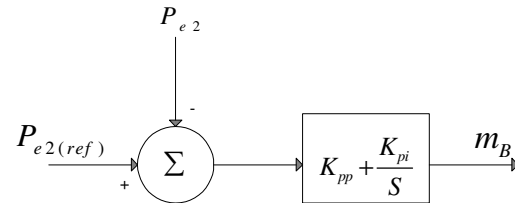


Fig. 3: Structure of power flow controller

5. Power System Stabilizer (PSS)

The main objective of designing PSS is to provide additional damping torque without affecting the synchronizing torque at critical oscillation frequency. The PSS [3] are designed to stabilize local and inter area modes. The transfer function block diagram of PSS is shown in Fig.4. which comprises of a gain block, signal washout and phase compensator. The dynamic compensator is made up of lead-lag stages having the following transfer function:

$$T(s) = \frac{K_{pss} (1 + sT_1)(1 + sT_3)}{(1 + sT_2)(1 + sT_4)} \quad (36)$$

where K_{pss} is the gain of PSS. The parameters of phase compensator are chosen so as to compensate the phase shift provided by the forward path of the closed loop system. The output of PSS must be limited to prevent the PSS acting to counter the action of Automatic Voltage Regulator (AVR). The gain setting of the damping controller is chosen such that, the desired damping of the electromechanical mode of concern is obtained, without affecting the damping of the other modes. The output of the damping controller modulates the reference setting of the power flow controller.

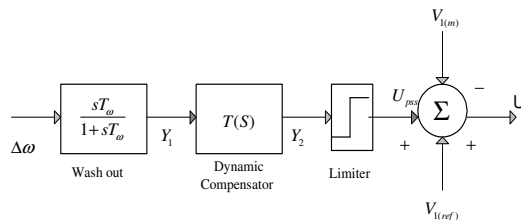


Fig.4: Transfer Function Block diagram of PSS

6. Optimization of Parameters using Nonlinear Control Design (NCD) Block Set

Various optimization techniques are available in literature for parameter optimization. However, trial and error method for parameters selection is very time consuming and less accurate whereas available optimization tool offers better result. The nonlinear control design block set in MATLAB uses the optimization tool box and it provides the simple approach to optimize model for given target output under define constraints and the define time intervals. The aim of the parameter optimization is

to achieve optimal performance. This objective can be formulated as follows [12]:

$$\text{Min } f(x) \quad (37)$$

$$\text{s.t. } A(x) = 0 \quad (38)$$

$$B(x) \geq 0 \quad (39)$$

where $f(x)$ is objective function, x are the parameters of the controllers. $A(x)$ are the equality functions and $B(x)$ are the inequality functions. Particularly $B(x)$ indicates the restriction of the parameters (i.e K_{pp} , K_{pi} etc.) The objective function in the simulation is defined as:

$$f(x) = \int_0^{t1} \omega(t, x) dt \quad (40)$$

where, $\omega(t, x)$ is the speed and the time range of the simulation. $\omega(t, x)$ changes by changing the parameters of x . The M file programme is employed to initialize NCD Block, to evaluate the performance of various parameters used in controllers. In the place of speed, rotor angle variation can also be used. The optimization starts with the pre-selected initial values of the feed back gains. Then the nonlinear algorithm is used iteratively to adjust the parameters, until the objective function equation (40) is minimized. These parameters so determined are the optimal setting of the parameters used as feedback gains. The flow chart of the parameter optimization is shown in Fig.5. The proposed optimization algorithm is realized in a single machine infinite bus system. Fig.6 shows the functional diagram of NCD for SMIB system with UPFC in which optimization of proportional & integral gain controller (K_{pp} & K_{pi}) has been done by NCD Blockset.

7. Simulation Results

7.1. Small Signal Stability Analysis with Damping Coefficient, $D=0$

Independent damping signals with UPFC during 10% of variation in mechanical power input has been demonstrated by using digital simulation with Modified Phillips Heffron model in MATLAB environment.

7.1.1. Dynamic performance of the system with control signal m_B

Result shown in Fig.7 indicates that with control signal m_B , exhibits negative damping. Also with coordinated tuning UPFC and PSS exhibits

relatively high peak, undamped oscillations whereas POD performance is improved with less settling time. Also, in the coordinated action of m_B and POD, when the value of proportional and integral setting are optimized, transient response is significantly improved.

This observation is verified by eigen value analysis of system wherein all the eigen values regarding POD migrate towards LHS of the complex plane while a pair of poles of PSS moves towards RHS of the complex plane as shown in Table 1.

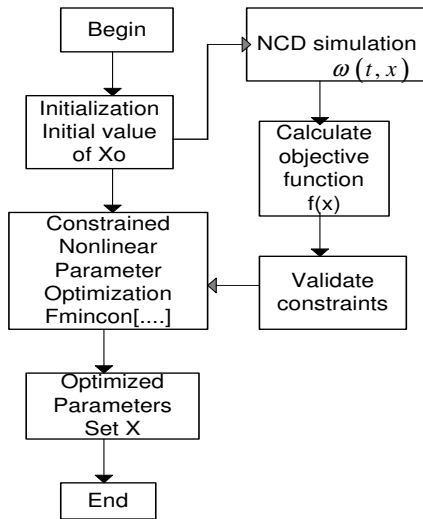


Fig.5: Flow chart of the parameters optimisation

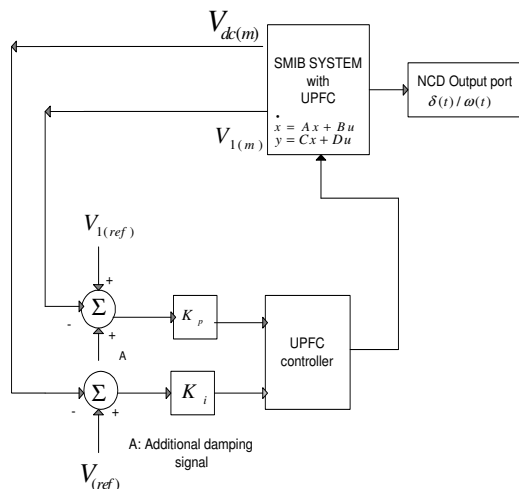


Fig.6. Functional diagram of UPFC parameters optimisation

7.1.2. Dynamic performance of the system with control signal m_E

From Fig.8 it is clear that with control signal m_E , system shows negative damping. Also system is not amenable with PSS indicates undamped oscillatory region, whereas POD Controller can suppress the oscillations well with settling time 0.25 sec. Also, in the coordinated action of m_E and POD, when the value of proportional and integral setting are optimized, transient response is significantly improved and hence gives the better result.

This observation is validated by coordinated action of UPFC with POD in which all the eigen values are driven into the negative real part of axis while one of the eigen values with coordinated action of UPFC with PSS is driven into the positive real part of axis as shown in Table 2.

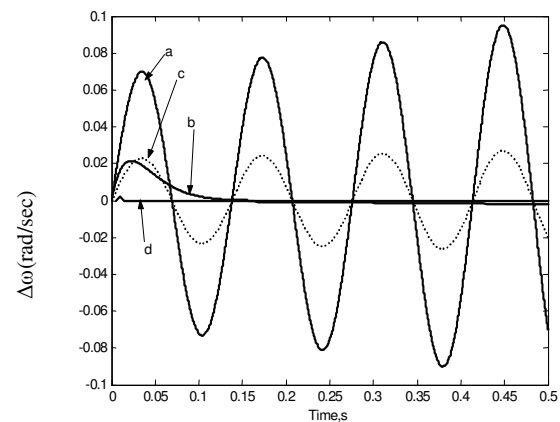


Fig.7:Dynamic response of linearized SMIB system
a. control signal m_B b. m_B with POD c. m_B with PSS
d. m_B with PSS

Table1: Eigen value analysis of linearized SMIB system with control signal m_B for $D=0$

Control signal m_B	with POD	with PSS
$0.75 \pm 45.57i$	$-41.72 \pm 13.79i$	$0.41 \pm 45.45.58i$
-0.00	-5.15	-4.54
-0.034	$-1.057 \pm 2.48i$	-4.54
$-1.057 \pm 2.48i$	-0.10	$-1.057 \pm 2.48i$
	-0.034	-0.00
	-0.00	-0.034
		-0.10

7.1.3. Dynamic performance of the system with control signal δ_B

From Fig. 9 it can be inferred that with coordinated tuning of UPFC and PSS, system is unstable, whereas POD performed well with settling time 0.2 sec. Also, in the coordinated action of δ_B and POD,

when the value of proportional and integral setting are optimized, transient response is significantly improved.

Table 3 shows the location of eigen values of the system wherein all the values with coordinated action of POD moves towards left half of the complex plane while one of the pair with the coordinated action of PSS moves towards right half of the complex plane which shows unstable oscillatory region.

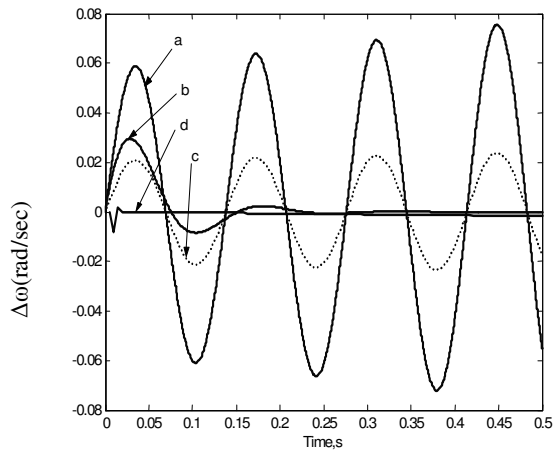


Fig.8:Dynamic response of linearized SMIB system
a. control signal m_E b. m_E with POD c. m_E with PSS
d. m_E with optimized POD

Table 2: Eigen value analysis of linearized SMIB system with control signal m_E for $D=0$

Control signal m_E	with POD	with PSS
$0.60 \pm 45.57i$	$-16.71 \pm 41.13i$	$0.33 \pm 45.58i$
-0.00	-5.98	$-4.54 \pm 0.00i$
-0.034	$-1.057 \pm 2.48i$	$-1.057 \pm 2.48i$
$-1.057 \pm 2.48i$	-0.10	0.00
	-0.034	-0.034
	0.00	-0.10

7.1.4. Dynamic performance of the system with control signal δ_E

Fig. 10 shows the instability of UPFC with PSS, whereas POD ensures better performance with less settling time. Also, in the coordinated action of δ_E and POD, when the value of proportional and integral setting are optimized, transient response is significantly improved and hence gives the better result.

Table 4 shows the eigen value analysis of system which shows that the all eigen values with

coordinated action of POD lies in the negative real part of the axis, hence ensures that system is stable while in case of PSS, a pair of pole will eventually migrate towards the RHS of the complex plane and maintains instability.

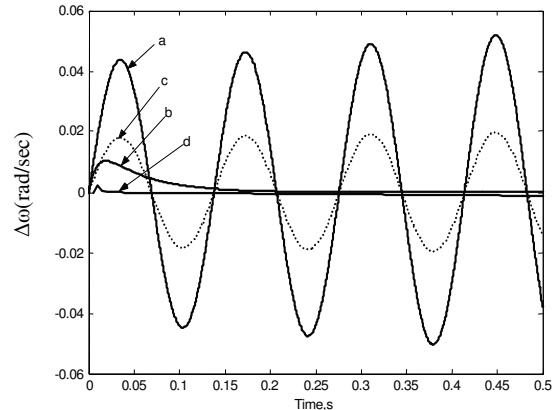


Fig.9:Dynamic response of linearized SMIB system
a. control signal δ_B b. δ_B with POD c. δ_B with PSS
d. δ_B with optimized POD

Table 3: Eigen value analysis of linearized SMIB system with control signal δ_B for $D=0$

Control signal δ_B	with POD	with PSS
$0.41 \pm 45.58i$	-106.93	$0.22 \pm 45.58i$
0.00	-20.41	-4.54
-0.034	-3.51	-4.54
$-1.057 \pm 2.48i$	$-1.06 \pm 2.49i$	$-1.057 \pm 2.48i$
	-0.10	-0.00
	-0.03	-0.034
	-0.00	-0.10

7.2. Small Signal Stability Analysis With Damping Coefficient, $D=4$

Digital Simulation has been carried out with Modified Phillips Heffron model in MATLAB environment. Independent damping signals, POD and PSS with UPFC has been demonstrated. The simulation result of the Modified Phillips Heffron model with four different input control signals under 10% of variation in mechanical power input is considered for analysis.

7.2.1. Dynamic performance of the system with control signal m_B

Result as shown in Fig.11 indicates that with the coordinated action of UPFC and PSS, first peak of

speed deviation is reduced with settling time 0.35 sec. whereas, with coordinated action of UPFC and POD Controller, first peak of speed deviation is reduced and steady state error has been significantly improved with settling time 0.1 sec. When the value of proportional and integral setting are optimized, the coordinated action of UPFC in coordination with Optimized POD Controller shows the highest improvement in transient response of the system. Table 5 shows the eigen value analysis of Single Machine Infinite Bus System system with UPFC in coordination with POD and PSS, in which all the eigen values lies on negative part of real axis which indicates that system is stable.

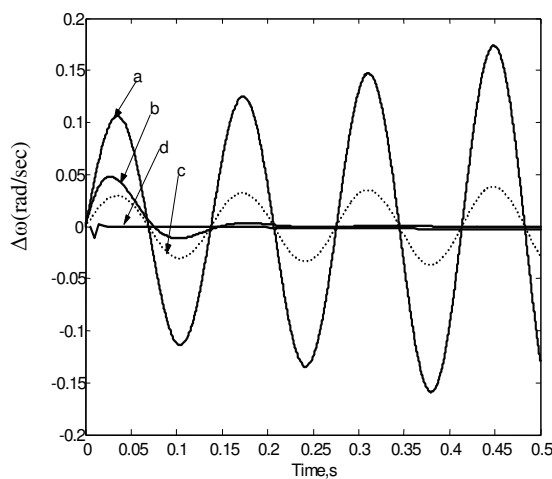


Fig.10:Dynamic response of linearized SMIB system
a. control signal δ_E b. δ_E with POD c. δ_E with PSS d. δ_E with optimized POD

Table 4: Eigen value analysis of linearized SMIB system with control signal δ_E for D=0

Control signal δ_E	with POD	with PSS
$1.20 \pm 45.56i$	$-18.69 \pm 41.72i$	$0.65 \pm 45.57i$
-0.00	-3.94	-4.54
-0.034	$-1.057 \pm 2.48i$	-4.54
$-1.057 \pm 2.48i$	-0.10	$-1.057 \pm 2.48i$
	-0.034	0.00
	0.00	-0.034
		-0.10

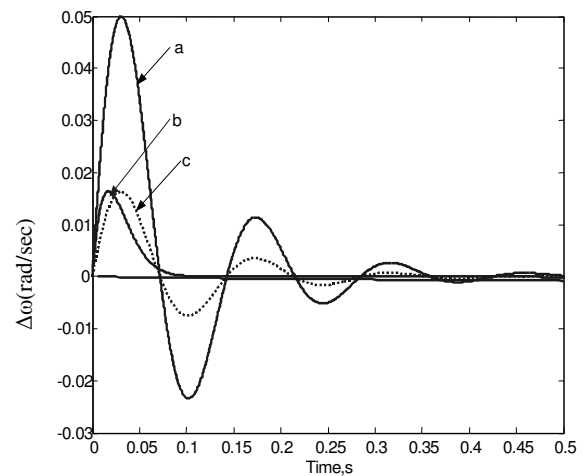


Fig.11:Dynamic response of linearized SMIB system
a. control signal m_B b. m_B with POD c. m_B with PSS d. m_B with optimized POD

Table5: Eigen value analysis of linearized SMIB system with control signal m_B for D=4

Control signal m_B	with POD	with PSS
$-10.43 \pm 43.98i$	$-53.40 \pm 32.34i$	$-10.77 \pm 44.080i$
-0.00	-4.22	$-4.54 \pm 0.00i$
-0.034	$-1.057 \pm 2.48i$	$-1.057 \pm 2.48i$
$-1.057 \pm 2.4857i$	-0.073	-0.00
	-0.027	-0.034
	0.00	-0.10

7.2.2. Dynamic performance of the system with control signal m_E

With coordinated action of UPFC and POD, reduction in peak amplitude, settling time and steady error are evident in Fig.12. With coordinated action of UPFC and PSS, first peak of speed deviation is reduced. Hence the coordinated action of UPFC with control signal m_E and Optimized POD Controller shows the improvement in the transient response of the system.

This inference has been checked by obtaining eigen value analysis of control signal m_E and coordinated tuning of POD Controller and PSS as shown in Table 6 in which all the eigen values lies on negative part of real axis which indicates that the system is stable.

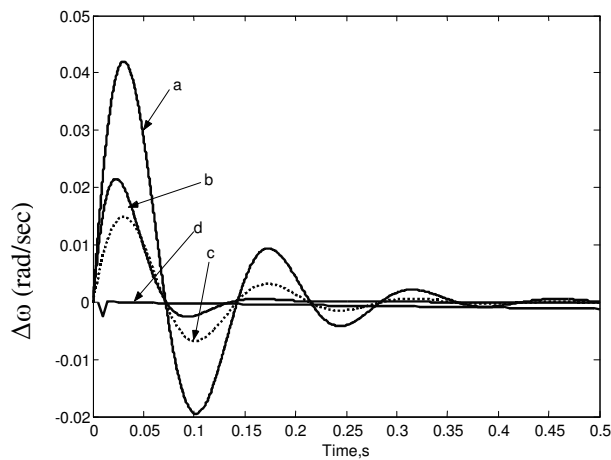


Fig.12:Dynamic response of linearized SMIB system
 a. control signal m_E b. m_E with POD c. m_E with PSS
 d. m_E with optimized POD

Table 6: Eigen value analysis of linearized SMIB system with control signal m_E for $D=4$

Control signal m_E	with POD	with PSS
$-10.58 \pm 44.028i$	$-28.39 \pm 44.30i$	$-10.85 \pm 44.10i$
-0.00	-5.029	$-4.54 \pm 0.00i$
-0.034	$-1.057 \pm 2.485i$	$-1.057 \pm 2.48i$
$-1.057 \pm 2.48i$	-0.089	-0.00
	-0.032	-0.034
	0.00	-0.10

7.2.3. Dynamic performance of the system with control signal δ_B

The digital simulation as shown in Fig.13 demonstrates the satisfied performance of coordinated effect of UPFC, POD Controller and PSS. Result indicates that the coordinated action of UPFC and Optimized POD Controller reduces first peak of speed deviation, settling time and steady state error has been significantly improved.

Result of eigen value computation is tabulated in Table 7 in which all the eigen values regarding coordinated action of UPFC with POD and PSS respectively lies on negative part of real axis which ensures that the system is stable.

7.2.4. Dynamic performance of the system with control signal δ_E

Result as shown in Fig.14 indicates that coordinated tuning of UPFC and Optimized POD Controller shows the improvement in the transient response of the system as compared with PSS.

This result can be confirmed by Table 8 which indicates that all the eigen values lies on negative part of real axis which ensures that system is stable.

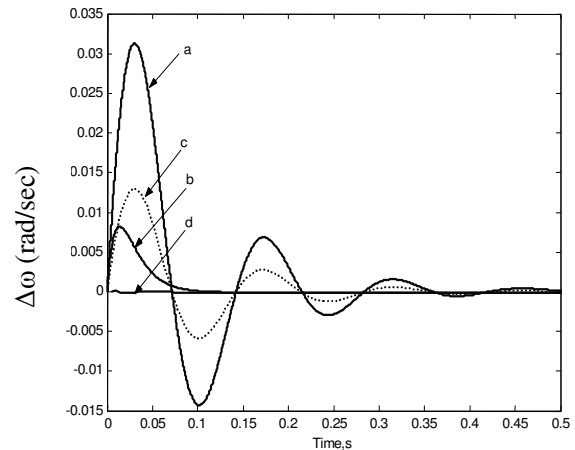


Fig.13:Dynamic response of linearized SMIB system a. control signal δ_B b. δ_B with POD c. δ_B with PSS d. δ_B with optimized POD

Table 7: Eigen value analysis of linearized SMIB system with control signal δ_B for $D=4$

Control signal δ_B	with POD	with PSS
$-10.77 \pm 44.080i$	-99.28	$-10.96 \pm 44.12i$
0.00	-49.91	-4.54
-0.034	-4.094	-4.54
$-1.057 \pm 2.48i$	$-1.057 \pm 2.48i$	$-1.057 \pm 2.48i$
	-0.072	-0.00
	-0.017	-0.034
	-0.00	-0.10

7.3. Small Signal Stability Analysis with Variation of Change in Mechanical Power

Simulation result of the Modified Phillips Heffron Model with independent tuning of POD Controller and PSS under zero damping coefficient and 20% deviation in mechanical power input has been demonstrated.

Control signals m_B and δ_B are more effective therefore they are considered for test under different system conditions.

7.3.1. Dynamic performance of the system with control signal m_B

Response shown in Fig. 15 indicates that Optimized POD Controller performance is far better than PSS with settling time 0.15 sec.

Eigen value analysis of system as shown in Table 1 indicates that results are similar as demonstrated for 10% deviation of mechanical power input.

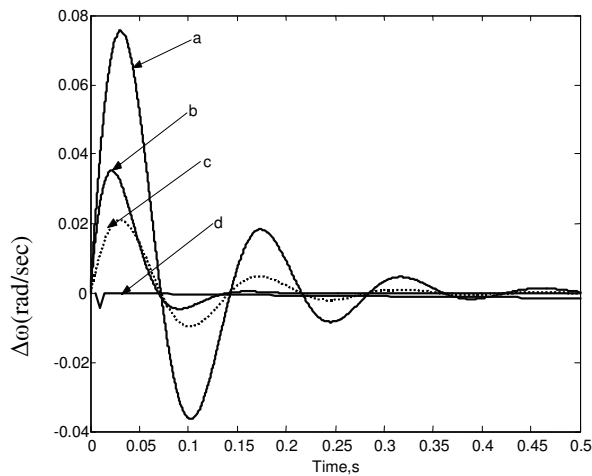


Fig.14: Dynamic response of linearized SMIB system

a. control signal δ_E b. δ_E with POD c. δ_E with PSS d. δ_E with optimized POD

Table 8: Eigen value analysis of linearized SMIB system with control signal δ_E for $D=4$

Control signal δ_E	with POD	with PSS
-9.99±43.86i	-29.83±45.07i	-10.53±44.014i
-0.00	-4.079	-4.54
-0.033	-1.057±2.48i	-1.057±2.48i
-1.057±2.48i	-0.078	-0.00
	-0.029	-0.034
	0.00	-0.100

7.3.2. Dynamic performance of the system with control signal δ_B

Response shown in Fig. 16 indicates that Optimized POD Controller provides highest improvement in stability. Eigen value analysis of system as shown in Table 3 indicates that results are similar as

demonstrated for 10% deviation of mechanical power input.

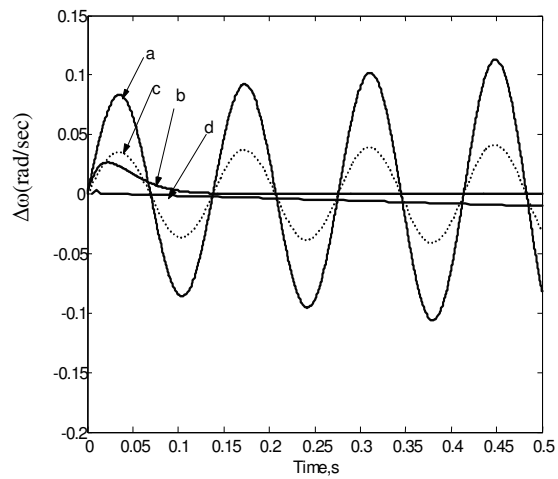


Fig.15: Dynamic response of linearized SMIB system with $D=0$ and $P_m=0.2$
a. control signal m_B b. m_B with POD c. m_B with PSS d. m_B with optimized POD

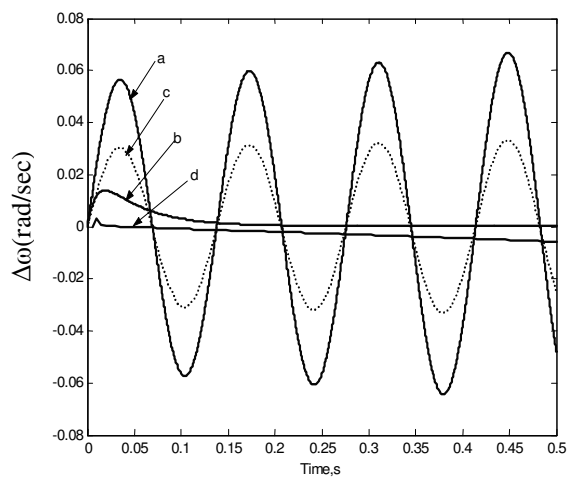


Fig.16: Dynamic response of linearized SMIB system with $D=0$ and $P_m=0.2$
a. control signal δ_B b. δ_B with POD c. δ_B with PSS d. δ_B with optimized POD

7.4. Small Signal Stability Analysis with Variation of Change in Mechanical Power

Simulation result of the Modified Phillips Heffron Model with independent tuning of POD Controller and PSS under 20% deviation in mechanical power input and damping coefficient=4 has been demonstrated. Control signals m_B and δ_B are more effective therefore they are considered for test under different system conditions.

7.4.1. Dynamic performance of the system with control signal m_B

Response shown in Fig. 17 indicates that POD Controller performance is far better than Power System Stabilizer with settling time 0.1 sec. Also, in the coordinated action of m_B and POD, when the value of proportional and integral setting are optimized, transient response is significantly improved and hence gives the better result. Eigen value analysis of system as shown in Table 5 indicates that results are similar as demonstrated for 10% deviation of mechanical power input.

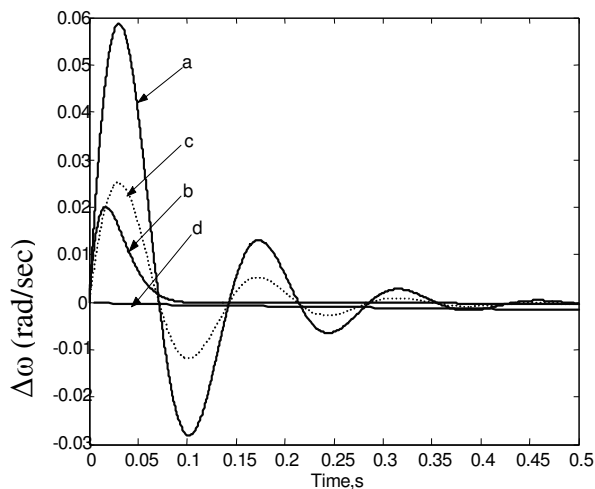


Fig.17: Dynamic response of linearized SMIB system with $D=4$ and $P_m=0.2$
a. control signal m_B b. m_B with POD c. m_B with PSS d. m_B with optimized POD

7.4.2. Dynamic performance of the system with control signal δ_B

Response shown in Fig. 18 indicates that POD Controller dynamic performance is improved than PSS with settling time 0.12 sec. Also, in the coordinated action of δ_B and POD, when the value of proportional and integral setting are optimized, transient response is significantly improved and hence gives the better result. Result also indicates that oscillations are completely damped.

With Eigen value analysis of system as shown in Table 7 indicates that results are similar as demonstrated for 10% deviation of mechanical power input and the damping coefficient $D=4$ which shows that all the eigen values regarding coordinated action of UPFC with POD and PSS respectively lies on negative part of real axis which ensures that the system is stable.

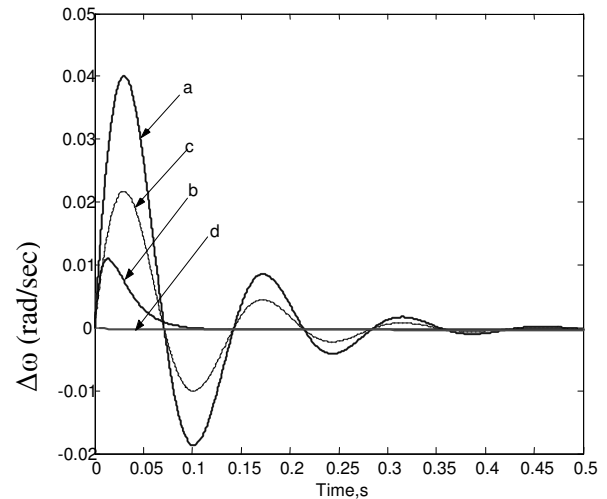


Fig.18: Dynamic response of linearized SMIB system with $D=4$ and $P_m=0.2$
a. control signal δ_B b. δ_B with POD c. δ_B with PSS d. δ_B with optimized POD

8. Conclusion

In this paper, the relative effectiveness of Unified Power Flow Controller (UPFC) control signals (m_E , δ_E , m_B , δ_B) in damping low frequency oscillations has been examined. The linearized power system model of Single Machine Infinite Bus system for analyzing the performance comparison of UPFC in coordination with Power Oscillation Damping (POD) Controller and Power System Stabilizer (PSS) has been considered. These control signals gives the significant improvement in performance of system for damping of power system oscillations. Investigations have revealed that UPFC control signals m_B and δ_B shows the robust performance over other signals. Also, POD Controller shows the improvement in transient response of the system as compared to PSS. Optimized system parameters further improves the transient response of the system. Optimized results of control signals m_B and δ_B in coordination with POD shows that oscillations are completely damped. Hence the series control signals are more effective than shunt control signals. The proposed controller fulfils the main objective of this paper. Time domain analysis and eigen value analysis results validated the performance of various Unified Power Flow Controller control strategy under variation of system parameters. This work can be continued with Artificial Intelligence (AI) application for improved dynamic performance.

Also optimal tuning method for multi-controller parameters can be implemented in large power system i.e. in multimachine system.

Acknowledgements

Authors are deeply indebted to Dept. of Electrical Engg., G. H. Raisoni College of Engineering for their constant support.

References:

- [1]N. G. Hingorani, L. Gyugyi, *Understanding FACTS: Concepts and Technology of Flexible AC Transmission Systems*, IEEE Power Engineering Society, IEEE press, Delhi, 2001.
- [2]Y.H.Song, A.T.Johns, *Flexible AC transmission systems (FACTS)*, IEE Power and Energy series 30, London, 1999.
- [3] K R Padiyar, *Power System Dynamics Stability and Control*, Interline Bangalore, 1996.
- [4]Wang H. F, Damping function of unified power flow controller, *IEE Proc. C Gener. Trans. Distrib.*, Vol. 146, No.1, 1999, pp 81-87
- [5]Wang H.F, A unified model for the analysis of FACTS devices in damping power system oscillations part III: unified power flow controller, *IEEE Trans. Power Delivery*, Vol.15, No.3, 2000, pp 978-983
- [6]N.Tambey & M. L. Kothari, Damping of power system oscillations with unified power flow controller (UPFC), *IEE Proc. Gen. Tran. & Distr.*, Vol.150, No.2, 2003, pp 129-140.
- [7]S.N.Dhurvey, V.K.Chandrakar, Damping of Power System Oscillations With Coordinated Tuning UPFC & POD, *Asian Power & energy System, IASTED*, Thailand, 2nd-4th April 2007, pp 270-275.
- [8]V.K.Chandrakar, A.G.Kothari, RBFN Based Unified Power Flow Controller (UPFC) for Improving transient stability performance, *WSEAS Transactions in power systems*, Vol.2, issue 1, Jan,2007, pp.1-6.
- [9]Anshul Chaudhary, Manish Jain, P.S. Venkataramu, T. Ananthapadmanabha, A Novel Method of UPFC Location Based on Sensitivity Factors, 7th WSEAS International Conference on power systems, Beijing, China, September 15-17, 2007, pp146-152.
- [10] Ashwani Kumar, Optimal Location of UPFC and Comparative Analysis of Maximum Loadability with FACTS In Competitive Electricity Markets, 7th WSEAS International Conference on Electric power

systems, High Voltages, Electric Machines, Venice, Italy, November 21-23, 2007, pp 59-66.

[11]Manisha Dubey, Aalok Dubey, Nikos E. Mastorakis, Simultaneous Stabilization of Multimachine Power system Using Genetic Algorithm Based Power System Stabilizers, 6th WSEAS/IASME International Conference on Electric Power Systems, High Voltages, Electric Machines, Tenerife, Spain, December 16-18, 2006, pp 208-213.

[12]MATLAB User's Manual, NCD Block Set, version 5.8.

Appendix-A

A.1. Generator

$$M=2H=0.1787, T_{do}^1=5.044, V_b=1 \text{ p.u.}$$

A.2. Excitation system

$$K_a=50.0, T_a=0.05$$

A.3.Constants

$$K_1=0.9849, K_2=4.0896, K_3=2.4422, K_4=0.1792, K_5=-0.0476, K_6=0.3514, K_7=-0.2697, K_8=0.2061, K_9=0.0397$$

A.4. Unified Power Flow Controller Parameters

$$K_{p\delta c}=1.0, K_{q\delta c}=0.5803, K_{v\delta c}=-0.0036, K_{c\delta c}=0.6206$$

$$K_{p\delta b}=-0.0089, K_{q\delta b}=-0.5388, K_{v\delta b}=-0.0029, K_{c\delta b}=0.0175$$

$$K_{pe}=0.3800, K_{qe}=-1.0858, K_{ve}=0.5468, K_{ce}=-0.0696,$$

$$K_{pd}=0.01931, K_{qd}=-0.5388, K_{vd}=0.2730, K_{pp}=1, K_{pi}=0.5$$

A.5.Controllability indices

$$\Delta m_B=0.0133, \Delta \delta_E=0.1916, \Delta m_E=0.4013, \Delta \delta_B=0.00036$$

For Damping controller m_B

$$K_{DC}=41.1419, T_1s=0.2860, T_2s=0.2082$$

For Damping controller m_E

$K_{DC}=14.8813$, $T_1s=0.3383$, $T_2s=0.1761$

For Damping controller δ_B

$K_{DC}=182.4410$, $T_1s=0.2266$, $T_2s=0.2694$

For Damping controller δ_E

$K_{DC}=18.0960$, $T_1s=0.2296$, $T_2s=0.2516$

6.PSS

$K_{pss}=21.31$, $T_o=10$, $T_1=0.31$, $T_2=0.22$, $K_{pp}=0.55$,
 $K_{pi}=0.75$